

# A Theoretical Analysis of the Unimolecular Decomposition of Ethanol: Internal Energy Effects and Pressure Dependence

Harrald V. Linnert\* and José M. Riveros

Instituto de Química, Universidade de São Paulo  
Caixa Postal 20780, 01498 São Paulo, SP, Brasil

Received: February 18, 1991; April 30, 1991

A decomposição unimolecular do etanol foi modelada de acordo com a teoria RRKM com o objetivo de comparar os dados obtidos a partir de excitação multifotônica vibracional e pirólise convencional. Três canais principais foram considerados: (1) eliminação de H<sub>2</sub>O, (2) ruptura da ligação C-C, e (3) ruptura da ligação C-O. Os cálculos de  $k(E^*)$  indicam claramente que o canal (1), de menor energia de ativação, é o predominante para energias de excitação até 85 kcal/mol. O comportamento previsto para  $k_{\text{uni}}$  em função da pressão revela que o processo de ruptura da ligação C-C deve ser o canal principal de reação, a pressões acima de 50 Torr, gerando um mecanismo radicalar.

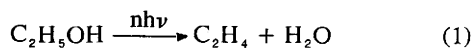
The unimolecular decomposition of ethanol has been modelled by RRKM theory to reconcile the data from infrared multiphoton excitation and conventional pyrolysis. Three main channels were considered: (1) H<sub>2</sub>O elimination; (2) C-C bond scission; and (3) C-O bond scission. The calculation of  $k(E^*)$  clearly predicts that the lowest activation energy channel (1) will be dominant up to excitation energies of 85 kcal/mol. The calculated behavior of  $k_{\text{uni}}$  as a function of pressure reveals that the C-C bond fission process leading to a free radical mechanism is expected to be the main channel at pressures above 50 Torr.

**Key words:** unimolecular processes, ethanol, RRKM theory.

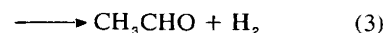
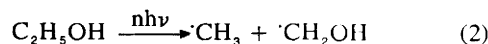
## Introduction

The use of methanol and ethanol in the neat or in mixtures as fuels has generated considerable interest in the understanding of their primary dissociation processes and the subsequent gaseous chemistry. The knowledge of the elementary reactions is essential in assessing the efficiency of the combustion processes and the environmental effects, both of which are presently a matter of controversy. While many reactions relevant to the combustion of methanol have been described<sup>1</sup>, several questions remain at large for the case of ethanol.

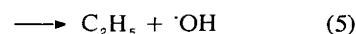
The pyrolysis of neat C<sub>2</sub>H<sub>5</sub>OH at 600°C and 185 Torr has been shown to yield mainly CH<sub>4</sub>, CO, CH<sub>3</sub>CHO and H<sub>2</sub> as the final products through a free radical process<sup>2</sup>. Non-kinetic experiments carried out at similar temperatures suggest a number of likely mechanisms to account for these products<sup>3,4</sup>. An alternative view of the primary processes in ethanol has been provided by the decomposition induced by vibrational multiphoton excitation with pulsed HF and CO<sub>2</sub> lasers<sup>5-10</sup>. The final product distribution displays a sensitive dependence on gas pressure (in the range of 100 mTorr to 40 Torr) and on laser energies: (a) ethylene is clearly the most abundant product at low pressures; (b) methane, carbon monoxide and hydrogen become increasingly important at the higher pressures and laser energies. Time resolved CARS experiments on nascent C<sub>2</sub>H<sub>4</sub> have unequivocally established ethylene as the product of a unimolecular reaction<sup>11</sup>.



Recent experiments<sup>10</sup> claim that under collisionless conditions IR laser MPD yields processes (1), (2) and (3) with a branching ratio of 0.68, 0.26 and 0.05 respectively.



Process (2) has been confirmed from laser experiments carried out in the presence of chlorine<sup>12</sup> and iodine<sup>13</sup> as radical scavengers, whereas reaction (3) has been inferred from studies with labelled ethanol<sup>13</sup>. Other possible dissociation channels, (4) through (6), have been considered in the laser driven combustion of ethanol<sup>14,15</sup>.



The diversity encountered between the pyrolysis and the laser driven reactions in ethanol, and the need to reconcile the existing data has prompted us to survey the behavior of the unimolecular pathways within the framework of RRKM theory. An earlier publication made use of RRKM calculations to predict the high pressure rate expressions for the decomposition of chemically activated alcohols<sup>16</sup>. A different approach to this problem has been reported by Yamabe *et al.*<sup>17</sup> based on ab initio MO calculations of the transition state topography for processes (1) and (2).

## Model for RRKM Calculations

The pyrolysis study of ethanol<sup>2</sup> yielded apparent activation energies and A factors from (i) the first order disappearance of C<sub>2</sub>H<sub>5</sub>OH, (ii) the total pressure increase.

The fact that these two methods result in different values clearly reflects the complexity of these reactions. An estimate for these two parameters for reaction (2) was proposed on the basis of single-pulse shock-tube experiments<sup>18</sup> of higher alcohols. However, the absence of reliable thermal data implies that the modelling of the possible unimolecular pathways requires suitable estimates of the activation energies and transition state geometries.

For the bond-fission processes, activation energies were chosen to be equal to the corresponding bond energies, i.e.  $E_2 = 82$  kcal/mol,  $E_4 = 90$  kcal/mol and  $E_5 = 85$  to  $92$  kcal/mol.<sup>19</sup> The value for  $E_1$  was estimated to be in the range of  $65$  to  $70$  kcal/mol by taking into account: (i) the empirical relationships that correlates activation energies for HX elimination in alkyl halides with heterolytic bond dissociation energies<sup>20</sup>, and (ii) the activation energy for H<sub>2</sub>O elimination in t-butanol<sup>21</sup>. An estimate for  $E_3$  and  $E_6$  is considerably more difficult because no similar systems are available in the literature that can be used as models. Yet, the fact that the theoretical calculations<sup>17</sup> predict  $E_3$  to be  $40$  kcal/mole higher than  $E_1$ , suggests that processes (3) and (6) may not be significant in the overall kinetics. Thus, no attempt was made to model these two reactions.

The vibrational frequencies for the transition states of the H<sub>2</sub>O elimination (1), the C-C bond rupture (2) and the C-O bond fission (5) were derived from the parent ethanol molecule<sup>22</sup>. The overall procedure was similar to that used in the case of ethyl chloride<sup>23</sup>. Frequencies were grouped to simplify the calculation of the sum of states according to the well established procedure in RRKM calculations<sup>24,25</sup>. Finally, several possibilities were considered for the number of free rotations in the transition state,  $r^\ddagger$ .

## Results

### A) Energy dependence of $k(E^*)$ for the Decomposition of Energized Ethanol.

The rate constants for reactions (1), (2) and (5), of energized ethanol,  $k(E^*)$ , were calculated as a function of

energy according to the known procedure outlined by Holbrook and Robinson<sup>25</sup>.

$$k(E^*) = L^\ddagger Q_1^\ddagger / Q_1 \{ \sum P(E_{v_r}^\ddagger) / hN(E^*) \}$$

where  $L^\ddagger$  = is the reaction path degeneracy;

$Q_1^\ddagger, Q_1$  = rotational partition function of the transition state and the reagent molecule;

$\sum_0^{E^* - E_0} P(E_{v_r}^\ddagger)$  = number of vibrational rotational states of the activated complex with internal energies above the critical energy for reaction  $E_0$ ;

$N(E^*)$  = density of vibrational rotational states of the energized molecule.

The parameters used to calculate  $k(E^*)$  for the three processes under consideration are shown in Table 1. For all cases, the transition state has been assumed to have one free rotation. The number of vibrational-rotational states and the density of states was calculated according to the method of Whitten and Rabinovitch<sup>26,27</sup>. The internal vibrational temperature was estimated to be  $1500$  K corresponding to the laser driven process. This amounts to the absorption of  $22$  photons and represents the threshold value compatible with the lowest activation energy for ethanol.

Figure 1 shows the variation of  $k(E^*)$  as a function of  $E^*$ .

### B) The Variation of $k_{uni}$ with Pressure.

Since the pyrolysis experiments are carried out at pressures where the experimentally measured rate constant corresponds to  $k_{uni}$  in the RRKM reaction scheme<sup>22</sup>, the second part of our work involved the computation of  $k_{uni}$  for the different channels. This rate constant is also

Table 1. Parameters of reactant molecule and complexes used in RRKM calculations for  $k(E^*)$ .

	Reactant molecule <sup>(a)</sup>		Transition state <sup>(b)</sup>	
	C <sub>2</sub> H <sub>5</sub> OH	H <sub>2</sub> O elimination	C-C bond fission	C-O bond fission
Vibrational frequencies (cm <sup>-1</sup> )	3676, 2989 (2) 2949, 2943 2901, 1490 1452 (2), 1451 1394, 1251 1241, 1089, 1062 1033, 885, 801 419, 234, 201	3106, 2946 (3) 1609 (2), 1453 (2) 1341 (2), 1246 (2) 1056 (3), 972 (2) 843 (2)	3676, 2954 (5) 1490, 1246 (2) 801, 726 (2) 702 (2), 530 (3) 111 (2)	3600, 3000 (2) 2800 (3), 1400 (2) 1000 (5), 500 (2) 250 (3), 200
$E_0$		64.3	77.1	80.2
$E_{v_r}^\ddagger$		30.7	17.9	14.8
$I/10^{-40}$ g cm <sup>2</sup>	23.05, 91.72, 105.6 <sup>(c)</sup>	26.2	182.6	25.6
$\log A/s^{-1}$		12.3	15.2	15.0
$r^\ddagger$		1	1	1
$L^\ddagger$		2	1	1
$\Delta S_{1500}^\ddagger$ K		-9.02	5.57	4.67

Critical energy,  $E_0$ , and energy for the activated complex,  $E_{v_r}^\ddagger$ , in kcal mol<sup>-1</sup>. Entropy of activation,  $\Delta S^\ddagger$ , in cal K<sup>-1</sup> mol<sup>-1</sup>.  $Z = 1.55 \times 10^7$  Torr<sup>-1</sup> s<sup>-1</sup>,  $\lambda = 1$ .  
(a) From<sup>22</sup>.

(b) Vibrational frequencies are based on the corresponding parent molecule and final product molecules or characteristics groups, so that desired A-factor is obtained. Transition state was viewed as the result of a diatomic dissociating into atoms with the masses of the fragments.

(c) From J.H.S. Green, *Trans. Faraday Soc.*, **57**, 2132 (1961).

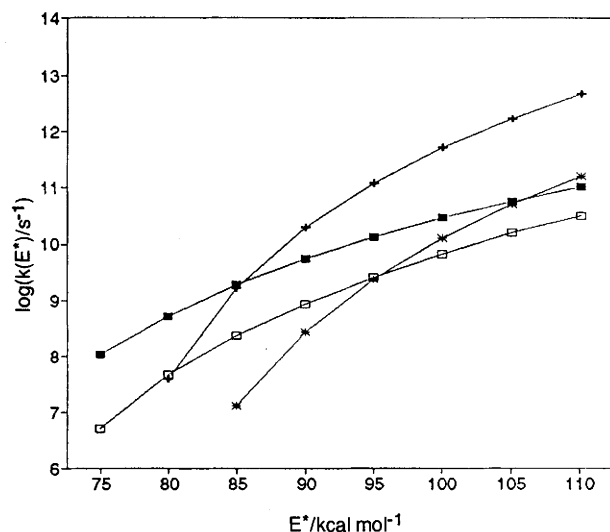


**Figure 1.** Variation of  $k(E^*)$  as a function of  $E^*$ .  $H_2O$  elimination,  $E_a = 65$  kcal/mol (■), C-C bond rupture (+), C-O bond rupture (\*),  $H_2O$  elimination,  $E_a = 70$  kcal/mol (□).

appropriate in the discussion of the laser promoted reaction at higher pressures (above 20 Torr) where the laser energization process is rapidly modulated by collisions. The unimolecular rate constant was calculated by using the expression where the RRKM integral is replaced by a sum in steps of small energy increases

$$k_{\text{uni}} = \frac{L^\ddagger Q_1^\ddagger \exp(-E_0/RT) \Delta E}{h Q_2} \sum_{i=1}^{i_{\text{max}}} \left[ \frac{\{\sum P(E_{\text{vr}}^+)\} \exp(-E^+/RT)}{1 + k(E^*)/\lambda Z_p} \right]$$

$$E^* = E_0 + E^+, \quad E^+ = (i + \frac{1}{2}) \Delta E^+$$

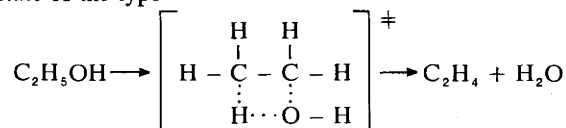
where  $Q_2$  = vibrational partition function of the reagent molecule, and

$\lambda Z_p$  = collisional deactivation rate constant.

Several models for the transition states were tested in this case as outlined in Table 2.

#### Model for $H_2O$ Elimination.

The reaction is assumed to proceed through a transition state of the type



for which  $L^\ddagger$  is 2,  $I \approx I^+$ , and  $Q_1^+/Q_1$  was taken to be unity in accord with a tight activated complex. It was assumed, in a first calculation, that there were no active rotations, and the vibrational contribution to the A-factor was  $\approx 10^{13} \text{ s}^{-1}$  at the temperature of 1500 K.

#### Models for C-C and C-O Rupture.

Three models, for the C-C rupture, illustrate the behaviour of the variation of  $k_{\text{uni}}$  with pressure, the A-factor and the number of internal rotation in the transition states.

Model I was viewed as the result of a diatomic transition state dissociating into atoms with the masses of the fragments. One internal rotation was considered for this transition state while six internal rotations are assumed for model II.

Model III correspond to the geometry of the free radicals obtained by the C-C bond rupture (tetrahedral  $\cdot CH_3$ , and  $\cdot CH_2OH$  based on the  $CH_3OH$  molecule)<sup>28,29</sup>, including six internal rotations for the transition state.

The model for C-O rupture corresponds approximately to a symmetric top  $C_2H_5$  radical and a diatomic OH radical. One internal rotation is assumed for the transition state.

The parameters for  $H_2O$  elimination, C-C and C-O bond rupture are shown in Table 2 while figure 2 shows the calculated values of  $\log k_{\text{uni}}$  as a function of pressure for the different models. The calculation of  $k_{\text{uni}}$  can be extrapolated to the typical pressures of 37.4 atm and temperatures of 2500 K encountered for ethanol and air in combustions chambers. Under these conditions the calculated rate constants become,  $k_{\text{uni}} = 2.33 \times 10^6 \text{ s}^{-1}$  for

**Table 2.** Parameters for  $H_2O$  elimination, C-C and C-O bond rupture in  $k_{\text{uni}}$  calculations.<sup>(a)</sup>

	Transition state <sup>(b)</sup>				
	$H_2O$ elimination	C-C bond rupture			C-O bond rupture
		model I	model II	model III	
Vibrational frequencies (cm <sup>-1</sup> )	3106, 2946 (3) 1609 (2), 1453 (2) 1341 (2), 1246 (2) 1056 (3), 972 (2) 843 (2), 201	3676, 2954 (5) 1490, 1246 (2) 801, 726 (2) 702 (2), 530 (3) 111 (2)	3100, 2100 (5) 300 (2), 200 (6)	1517, 759 (2) 657 (3), 527 (2) 329 (2), 266 (4)	3114, 2100 (5), 1442 726 (3), 500 (3) 419 400, 250 (4)
$E_0/\text{kcal mol}^{-1}$	63.1	77.1	73.4	67.9	75.2
$E_{\text{vr}}^\ddagger/\text{kcal mol}^{-1}$	31.9	17.9	21.6	27.1	19.8
$1/10^{-40} \text{ g cm}^2$		182.6	182.6	40.65, 36.56, 9.43	6.73, 4.92, 4.92
$\log A/\text{s}^{-1}$	13.4	15.2	15.4	16.4	16.8
$r^\ddagger$	0	1	6	6	1
$L^\ddagger$	2	1	1	1	1
$\Delta S_{1500 \text{ K}}^\ddagger / \text{cal K}^{-1} \text{ mol}^{-1}$	-3.73	5.57	6.89	11.07	13.48

$\lambda = 1$ ;  $Z = 1.55 \times 10^7 \text{ Torr}^{-1} \text{ s}^{-1}$ .

(a) Reactant molecule parameters equal Table 1.

(b) Vibrational frequencies are based on the corresponding parent molecule and final product molecules or characteristics groups, so that desired A-factor is obtained.

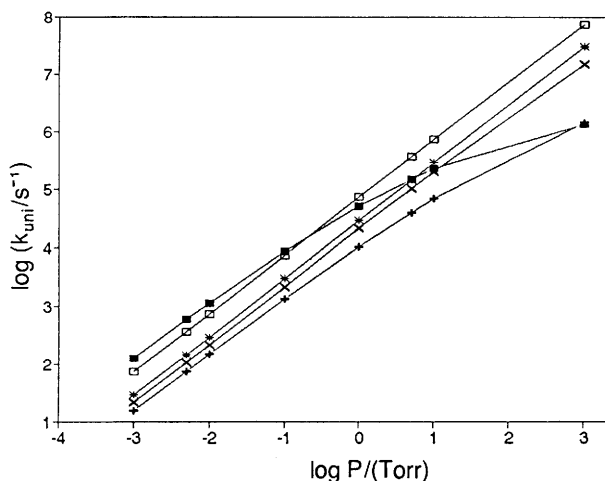


**Figure 2.** Calculated values of  $\log k_{uni}$  as a function of pressure.  $H_2O$  elimination (■), C-C bond rupture, model I (+), C-C bond rupture, model II (\*), C-C bond rupture, model III (□), C-O bond rupture (x).

water elimination,  $k_{uni} = 2.23 \times 10^9 \text{ s}^{-1}$  for C-C bond rupture, and  $k_{uni} = 4.31 \times 10^{10} \text{ s}^{-1}$  for C-O bond rupture. While it is difficult to assess the reliability of these predictions in a combustion chamber in an air/ethanol mixture and under turbulent conditions, it is interesting to notice the tendency of the C-O bond fission to become the predominant channel.

## Discussion

The calculations performed in this work clearly help to understand the outcome of the laser experiments, at low and high pressures, and the observations under pyrolytic conditions.

The results of  $k(E^*)$  as a function of energy for example show that the C-C bond rupture will begin to be the dominant mechanism at internal energy contents above 85 kcal/mol. This is in agreement with experiments<sup>9</sup> using a shorter  $CO_2$  laser pulse at constant laser fluence. While the exact energy at which the crossover occurs will be dependent on the particular models which are used, the trend is not appreciably changed by variations of the transition state parameters. It is also noticeable that the process involving C-O bond rupture is always predicted to be a minor channel in agreement again with experiments which fail to detect final products that could be explained from this mechanism.

While the laser experiments are best analyzed by observing the variation of  $k(E^*)$ , the pyrolysis experiments and the pressure behavior of the laser induced MPD are best compared to the trends shown in Figure 2. Although significant differences can be observed depending on the model used for the transition states, it is clear that the calculations predict that at pressures above 100 Torr the radical initiated reactions will overshadow the elimination process. This is in qualitative agreement with the pyrolysis experiments for which the final products originate from free radical reactions initiated by reactions (3) and (5)<sup>2-4</sup>. The product distribution of the laser induced process at pressures above 10 Torr also reveals the relative growth of CO and  $CH_4$  (products due to free radical reactions) as mentioned in the introduction<sup>9</sup>. The fact that even the laser promoted decomposition at higher pressures favors

the bond fission process, is clearly due to the fact that collisions are more effective in relaxing the energized species with longer lifetimes, i.e. those with lower energy content and unable to undergo dissociation prior to collision.

The calculated behavior capable of reproducing the trend of both the thermal and laser experiments also points out that the model outlined here for the primary dissociation processes of ethanol is correct. While considerable improvements could be proposed for the calculations of  $K(E^*)$ <sup>30</sup> and  $k_{uni}$ <sup>31</sup> such procedures are not justified at present in the absence of reliable experimental values for the A factors and the activation energies.

While we have neglected to consider the possible contribution of reaction (3) due to the difficulty in estimating the activation energy, it is questionable whether this process can compete effectively with the other elimination channel. Since this reaction also involves a tight transition state, the expected A factor would be in the range of  $10^{13} \text{ s}^{-1}$ . Given the higher activation energy expected for this path, it is unlikely that this process could be very effective in becoming a dominant channel at higher energies or higher pressures.

Our present work is a good example of how RRKM calculations can help not only in understanding the primary dissociation channels of important molecules but also in bridging the gap between low pressure laser driven reactions and high pressure pyrolysis.

## Acknowledgments

This work was made possible by the continuous support of Fundação de Amparo à Pesquisa do Estado de São Paulo (FAPESP), the Conselho Nacional de Pesquisas (CNPq), and the Financiadora de Estudos e Projetos (FINEP).

## References

1. C.K. Westbrook, F.L. Dyer, *Combust. Sci. Tech.* **20**, 125-140 (1979).
2. J.A. Barnard, H.W.D. Hughes, *Trans. Far. Soc.* **56**, 55-63 (1960).
3. B.C. Capelin, G. Ingram, J. Kokolis, *Microchem. J.* **19**, 229-252 (1974).
4. G. Ingram, S.M.H. Rizvi, *Microchem. J.* **19**, 253-271 (1974).
5. L. Sewyn, R.A. Back, C. Willis, *Chem. Phys.* **32**, 323-328 (1978).
6. W.C. Dancn, *J. Am. Chem. Soc.* **101**, 1187-1190 (1982).
7. A. Gandini, R.A. Back, *J. Photochem.* **18**, 241-244 (1982).
8. S.R.A. Leite, P.C. Isolani, J.M. Riveros, *Can. J. Chem.* **62**, 1380-1384 (1984).
9. R.A. Back, D.K. Evans, R.D. McAlpine, E.M. Verpoorte, M. Ivanco, J.W. Goodale, H.M. Adams, *Can. J. Chem.* **66**, 857-865 (1988).
10. G.P. Zhitneva, I.A. Mackina, S.A. Pshezhetskü, *Laser Chem.* **8**, 259-274 (1988).
11. P.C. Isolani, J.M. Riveros, E.L. Schweitzer, J.I. Steinfeld, *MIT Laser Research Center Summary Report*, 1985, 23.
12. H.V. Linnert, *Doctoral Thesis*, University of São Paulo, 1989.
13. J.W. Goodale, D.K. Evans, M. Ivanco, R.D. McAlpine, *Can. J. Chem.* **68**, 1437-1439 (1990).
14. J.M. Riveros, P.C. Isolani, S.R.A. Leite, *Chem. Phys. Lett.* **99**, 442-444 (1983).
15. P.C. Isolani, H.V. Linnert, J.M. Riveros, J.F.G. Faigle, *An. Acad. bras. Ci.* **57**, 522 (1985).
16. W. Tsang, *Int. J. Chem. Kinet.* **8**, 193-203 (1976).

17. T. Yamabe, M. Koizumi, K. Yamashita, A. Tachibana, *J. Am. Chem. Soc.* **106**, 2255-2260 (1984).
18. W. Tsang, *Int. J. Chem. Kinet.* **8**, 173-192 (1976).
19. S.W. Benson, *Thermochemical Kinetics*, 2nd. Edn. (John Wiley & Sons, New York, 1976).
20. W. Tsang, *J. Chem. Phys.* **41**, 2487-2494 (1964).
21. W. Tsang, *J. Chem. Phys.* **40**, 1498-1505 (1964).
22. A.J. Barnes, H.E. Hallam, *Trans. Far. Soc.* **66**, 1932-1940 (1970).
23. J.C. Hassler, D.W. Setser, *J. Chem. Phys.* **45**, 3246-3257 (1966).
24. B.S. Rabinovitch, D.W. Setser, *Adv. Photochem.* **3**, 1-82 (1964).
25. P.J. Robinson, K.A. Holbrook, *Unimolecular Reactions* (Wiley-Interscience, Bristol, England, 1972).
26. G.Z. Whitten, B.S. Rabinovitch, *J. Chem. Phys.* **41**, 1883 (1964).
27. D.C. Tardy, B.S. Rabinovitch, G.Z. Whitten, *J. Chem. Phys.* **48**, 1427-1429 (1968).
28. H.S. Johnston, *Advan. Chem. Phys.* **3**, 133-170 (1961). G. Herzberg, *Proc. Roy. Soc. London A262*, 291, (1961).
29. M.E. Jacox, D.E. Milligan, *J. Molec. Spectrosc.* **47**, 148-162 (1973). G. Herzberg, *Molecular Spectra and Molecular Structure II. Infrared and Raman Spectra of Polyatomic Molecules*. D van Nostrand, (N.Y., 1945) p. 335. A. Borden, E.F. Barker, *J. Chem. Phys.* **6**, 553-563 (1938).
30. L. Brouwer, C.J. Cobos, J. Troe, H.-R. Dubal, F.F. Crim, *J. Chem. Phys.* **86**, 6171-6182 (1987).
31. R.E. Weston, Jr., *Int. J. Chem. Kin.* **18**, 1259-1276 (1986).